Structure of Solvation Sphere of Tris(acetylacetonato)chromium(III) in Acetonitrile

Mitsuhiro Kanakubo,[†] Haruko Ikeuchi,*[,†] Gen P. Satô,[†] and Haruhiko Yokoyama[‡]

Department of Chemistry, Faculty of Science and Technology, Sophia University, 7-1 Kioicho, Chiyoda-ku, Tokyo 102, Japan, and Department of Chemistry, Yokohama City University, 22-2 Seto, Kanazawa-ku, Yokohama 236, Japan

Received: October 29, 1996; In Final Form: February 5, 1997[⊗]

Two experimental techniques were used to elucidate how acetonitrile molecules are bound to the title complex, $[Cr(acac)_3]$: (i) measurement of NMR longitudinal relaxation rates of the dipolar nuclei of the solvent (^1H, methyl-^{13}C, and cyano-^{13}C of CH_3CN) in the presence of $[Cr(acac)_3]$, which is a paramagnetic complex, and (ii) X-ray diffraction measurements on acetonitrile solutions of $[Cr(acac)_3]$ and $[Ru(acac)_3]$ using an isostructural substitution method. The results of both methods are in harmony with each other. Four acetonitrile molecules are found within about 6×10^{-10} m from the chromium atom. They are in the hollows on the peripheral surface of the three acetylacetonato ligands, one or two in the hollows along the C_3 axis of the complex, and two or three in the hollows along the C_2 axes. They are oriented with the methyl ends inward: the angle between the molecular axis of acetonitrile and the vector from the chromium atom to the methyl carbon of acetonitrile was about 100°.

I. Introduction

Quite a few studies have been reported on the solvation structure of neutral complexes of which the first coordination sphere is occupied with stable ligands, since solute−solvent interactions in such systems are generally weak and it is often difficult to draw any clear picture by means of a single method. In the present paper, we describe how acetonitrile molecules are bound to tris(acetylacetonato)chromium(III), as studied by combining NMR and X-ray diffraction methods.

Tris(acetylacetonato)chromium(III) (Figure 1), $[Cr(acac)_3]$ ($acac^- =$ 2,4-pentanedionate ion), is chosen as the solute, because it is an inert, stable, and paramagnetic complex quite soluble in acetonitrile. Moreover, structurally very similar analogs of cobalt(III) and ruthenium(III) are available; the former is a good diamagnetic partner for NMR relaxation rate measurements,[1,2] and the latter serves as a suitable isostructural partner[3,4] for the isomorphous substitution technique of the solution X-ray diffraction method.[5,6] These molecules are almost spherical except for having five hollows (two along the C_3 axis and three along the C_2 axes). These hollows aside, the peripheries are hydrocarbons. If acetonitrile molecules are bound to the complex, they are likely to be accommodated in these hollows.

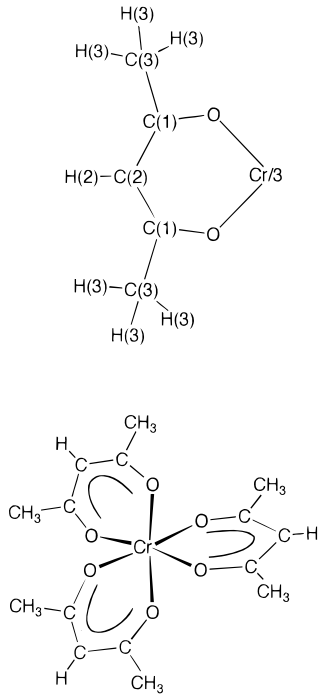

Figure 1. Tris(acetylacetonato)chromium(III).

II. Theoretical Background

A. NMR Relaxation Rate in the Presence of a Paramagnetic Complex. When a solution contains a paramagnetic complex, the observed relaxation rate, $R_{1,obs}$, of a nucleus of a solvent is generally expressed by[7]

$$R_{1,obs} = R_1^{e} + R_1^{dia} \quad (1)$$

where R_1^e is the rate of the relaxation through the interaction of the nuclear magnetic dipole with the magnetic dipole of the unpaired electron(s) of the complex, and R_1^{dia} is the rate of the relaxation through diamagnetic interactions.

We assume that the solvent molecules are either "bound" or "free". The bound solvent molecules are fixed on the paramagnetic complex molecules, and their nuclei relax with a rate of R_1^e(bound) as they rotate together with the complex molecules. The nuclei of the free solvent molecules relax with a rate of R_1^e(free) when the solvent molecules change position relative to the complex molecules. Here we neglect the effect of the exchange between the bound and free solvent molecules on the nuclear relaxation. The picture of a single bound state is certainly an oversimplification, because a $[Cr(acac)_3]$ molecule has two kinds of hollows, as mentioned in the previous section. In fact, the present X-ray diffraction study suggests two kinds of bound solvent molecules (see section IV.B). Nevertheless, this simplified model is more practical for the analysis of NMR relaxation rates than the two-kind model, which might impair

[†] Sophia University.
[‡] Yokohama City University.
[⊗] Abstract published in *Advance ACS Abstracts,* April 15, 1997.

S1089-5647(96)03356-1 CCC: $14.00 © 1997 American Chemical Society

the analysis by introducing too many unknowns, and the inferences based on it will provide meaningful information about the average state of the bound solvent molecules.

If the fraction x of the solvent molecules are bound,

$$R_1^{\,e} = xR_1^{\,e}(\text{bound}) + (1 - x)R_1^{\,e}(\text{free}) \tag{2}$$

By expressing x in terms of the concentration (molarity) of the complex, c, eq 1 for a dilute solution, where $1 - x \approx 1$, becomes

$$R_{1,\text{obs}} = \frac{Nc}{c_s}R_1^{\,e}(\text{bound}) + R_1^{\,e}(\text{free}) + R_1^{\,\text{dia}} \tag{3}$$

where N is the average number of bound solvent molecules per complex molecule and c_s is the total concentration of the solvent. The last term of the right-hand side is expected to be the same as the relaxation rate observed in the absence of the paramagnetic complex. Expressions of the first two terms suitable to the present system are derived as follows.

Expressions of $R_1^{\,e}$(bound) and $R_1^{\,e}$(free). The longitudinal relaxation rate of a dipole nucleus that interacts with the magnetic dipole of unpaired electrons, whose total electron spin quantum number is S, is given by[8]

$$R_1 = K_I\{(^1/_{12})J_0(\omega_I - \omega_S) + (^3/_2)J_1(\omega_I) + (^3/_4)J_2(\omega_I + \omega_S)\} \tag{4}$$

with

$$K_I = (\mu_0/4\pi)^2\,\gamma_I^{\,2}\gamma_S^{\,2}\,S(S+1)\hbar^2 \tag{5}$$

Here, the subscript I refers to the dipole nucleus and S to the electrons, γ is the magnetogyric ratio, ω is the angular frequency of the Lamor precession, μ_0 is the permeability of vacuum, and J_0, J_1, and J_2 are the spectral density functions. For common nuclides $\omega_I \ll \omega_S$, and eq 4 reduces to

$$R_1 = K_I\{(^1/_{12})J_0(\omega_S) + (^3/_2)J_1(\omega_I) + (^3/_4)J_2(\omega_S)\} \tag{6}$$

where $J_0(-\omega_S) = J_0(\omega_S)$ by definition.

The explicit forms of the spectral density functions are obtained on the following assumptions: (i) the translational and rotational motions of the solvent and complex molecules are described by the Brownian motion model with the Debye approximation,[9] and (ii) the relaxation of the unpaired electrons does not affect the spectral density functions. The second assumption seems to hold in the present case, because the electron spin relaxation time is approximately 10^{-9} s for [Cr(acac)$_3$][10,11] and the translational and rotational correlation times are about 10^{-11} s in acetonitrile solutions.

The spectral density functions for the rotational motion are given by[8]

$$J_0(\omega) = \frac{24}{15}\frac{1}{r^6}\frac{\tau_r}{1+\omega^2\tau_r^{\,2}}, \quad J_1(\omega) = \frac{4}{15}\frac{1}{r^6}\frac{\tau_r}{1+\omega^2\tau_r^{\,2}}, \quad J_2(\omega) = \frac{16}{15}\frac{1}{r^6}\frac{\tau_r}{1+\omega^2\tau_r^{\,2}} \tag{7}$$

Here, τ_r is the rotational correlation time of the complex molecule to which solvent molecules are bound and r is the distance between the nucleus of the bound solvent molecule and the total electron spin. In the case of [Cr(acac)$_3$], the total electron spin resides at the chromium atom because of the symmetrical distribution of three unpaired electrons. Substitution of eqs 7 into eq 6 gives R_1 for the nucleus of the bound solvent:

$$R_1^{\,e}(\text{bound}) = K_I\frac{1}{r^6}\left\{\frac{6}{15}\frac{\tau_r}{1+\omega_I^{\,2}\tau_r^{\,2}} + \frac{14}{15}\frac{\tau_r}{1+\omega_S^{\,2}\tau_r^{\,2}}\right\} \tag{8}$$

This expression can be simplified in the present experiment as

$$R_1^{\,e}(\text{bound}) = K_I\frac{2}{5r^6}\tau_r \tag{9}$$

because $\omega_H = 1.7 \times 10^9$ Hz, $\omega_C = 4.3 \times 10^8$ Hz, and $\omega_S = 1.1 \times 10^{12}$ Hz at a magnetic flux density of 6.34 T, and $1/\tau_r \approx 10^{11}$ Hz.

The spectral density functions for the translational motion are given by Hubbard:[12]

$$J_0(\omega) = \frac{48\pi}{15}\frac{N_A c}{dD_t}U(\omega), \quad J_1(\omega) = \frac{8\pi}{15}\frac{N_A c}{dD_t}U(\omega), \quad J_2(\omega) = \frac{32\pi}{15}\frac{N_A c}{dD_t}U(\omega) \tag{10}$$

with

$$U(\omega) = \frac{u^2 - 2 + e^{-u}[(u^2-2)\sin u + (u^2+4u+2)\cos u]}{u^5} \tag{11}$$

where

$$u^2 = \omega d^2/D_t \tag{12}$$

Here, N_A is the Avogadro constant, d is the minimum distance of approach between the chromium atom and the nucleus of the free solvent, and D_t is the arithmetic mean of the translational diffusion coefficients of the complex and solvent molecules. Obviously U tends to u^{-3} for $1 \ll \omega d^2/D_t$, and it tends to 2/15 for $\omega d^2/D_t \ll 1$. In the present case, $\omega_I d^2/D_t \ll 1 \ll \omega_S d^2/D_t$, and it follows that

$$J_0(\omega_S) = \frac{48\pi}{15}\frac{N_A c D_t^{\,1/2}}{d^4\omega_S^{\,3/2}}, \quad J_1(\omega_I) = \frac{16\pi}{225}\frac{N_A c}{dD_t}, \quad J_2(\omega_S) = \frac{32\pi}{15}\frac{N_A c D_t^{\,1/2}}{d^4\omega_S^{\,3/2}} \tag{13}$$

Among these three, only $J_1(\omega_I)$ is significant because $1/dD_t \approx 10^{18}$ m^{-3} s and $D_t^{1/2}/d^4\omega_S^{3/2} \approx 10^{14}$ m^{-3} s. Consequently, the expression of $J_1(\omega_I)$ in eq 13 is introduced into eq 6 to give

$$R_1^{\,e}(\text{free}) = K_I\frac{8\pi}{75}\frac{N_A c}{dD_t} \tag{14}$$

B. X-ray Diffraction on Isostructural Solutions of Metal Complexes. Radial distribution functions were derived according to the manner previously described.[5,6] The experimental radial distribution function, $D(r)$, involving all two-atoms correlations in solution was obtained by

$$D(r) = 4\pi r^2\rho_0 + \frac{2r}{\pi}\int_0^{s_{\max}} si(s)\,M(s)\sin(rs)\,ds \tag{15}$$

where $\rho_0 = (\sum n_i Z_i)^2/V$, $s = 4\pi(\sin\theta)/\lambda$, $i(s)$ is the reduced intensity, and $M(s)$ is the modification function with the scattering factor of oxygen (f_o) and a damping factor $k = 0.01 \times 10^{-20}$ m^2, that is, $M(s) = (f_o(0)/f_o(s))^2\exp(-ks^2)$. n_i is the number of atoms i with atomic number Z_i in V, which is the stoichiometric unit volume including one complex molecule, and the other symbols have their usual meanings. The radial

distribution function, $D^{M}(r)$, involving only metal correlations such as M−O, M−C, and so on was obtained by

$$D^{M}(r) = 4\pi r^2 \rho_0^{M} + \frac{2r}{\pi}\int_0^{s_{max}} s\Delta i(s)\, F(s)\, M(s) \sin(rs)\, ds \quad (16)$$

with

$$F(s) = \frac{f_M(s)}{f_M(s) - f_{M'}(s)} \quad (17)$$

where ρ_0^{M} corresponds to the terms concerning the metal M in ρ_0, $F(s)$ is the deconvolution factor, and $\Delta i(s)$ is the difference of reduced intensities between the M complex solution and the M′ complex solution.

The theoretical intensity, $i_{M-q}(s)$, for the correlation between the atoms M and q was given by

$$i_{M-q}(s) = 2n_q f_M(s)\, f_q(s) \frac{\sin\{r(M-q)s\}}{r(M-q)s} \exp\left(-\frac{l^2 s^2}{2}\right) \quad (18)$$

where n_q is the number of atoms q in V and l is the root mean square variation of the distance r(M−q). The contribution to $D(r)$ by the M−q correlation is given by

$$D_{M-q}(r) = \frac{2r}{\pi}\int_0^{s_{max}} s i_{M-q}(s)\, M(s) \sin(rs)\, ds \quad (19)$$

The analysis of $D^{M}(r)$ was made by use of the following equation, since a small difference was found between r(Ru−O) and r(Cr−O), as described later.

$$D_{M-q}(r) = \frac{2r}{\pi}\int_0^{s_{max}} s\{i_{M-q}(s) - i_{M'-q}(s)\} F(s)\, M(s) \sin(rs)\, ds \quad (20)$$

where M stands for Ru and M′ for Cr.

III. Experimental Section

A. NMR Experiments. The sample of [Cr(acac)$_3$] obtained from Dojindo Laboratories, after being purified by means of alumina column chromatography with CH_2Cl_2, was dried under a reduced pressure for a few days. Reagent-grade CH_3CN was purchased from Wako Pure Chemical Industries, Ltd., and purified as previously described.[13] The water content of the purified solvent was less than 6 mol m^{-3}, as determined with a Karl-Fischer moisture meter. NMR sample tubes were of a conventional double-tube type. Every sample solution was degassed by several freeze−pump−thaw cycles and then sealed into the inner tube under vacuum. Chloroform-*d* in the outer tube was used for NMR lock solvent and for the reference.

The molality, m, of the complex in the sample solution was determined from the linear dependence of the ^{1}H chemical shift of CH_3CN on m ($d\delta(^1H)/dm = 0.019\,62$ mmol^{-1} kg at 298.8 K). The concentration was calculated from m by using the density of pure solvent and the partial molar volume of [Cr(acac)$_3$] in CH_3CN, which was determined to be 267 cm^3 mol^{-1} from the measurements of densities of the complex solutions for $c < 0.1$ mol dm^{-3} at 298 K. The partial molar volume was considered to be independent of temperature, as is the case for similar complexes.[14] The values of c are listed in Table 1.

Each NMR measurement was made on a JEOL GX-270 spectrometer. The relaxation rates were determined by the conventional inversion recovery method with a pulse sequence of [180°−t−90°(detect)−PD], where t is the variable delay and PD is the pulse delay ($>5/R_{1,obs}$). In the case of the ^{13}C experiment, the protons were decoupled. The temperature was controlled within ±0.1 K by a JEOL NMGV-T3 temperature control unit. Temperature readings of the controller were previously calibrated.[1]

TABLE 1: Concentrations of [Cr(acac)$_3$] of the Sample Solutions (mol m^{-3})

		T (K)		
sample number	m (mmol kg^{-1})	278.9	298.8	318.7
0	0	0	0	0
1	7.9	6.3	6.1	6.0
2	16.3	13.0	12.6	12.3
3	29.2	23.1	22.5	21.9
4	45.3	35.7	34.8	33.8
5	53.8	42.4	41.3	40.1
6	67.3	52.9	51.5	50.1
7	97.5	76.2	74.2	72.2
8	128.2	99.4	96.8	94.2

TABLE 2: Concentrations (c), Densities (d), Stoichiometric Unit Volumes (V), and Absorption Coefficients (μ) of Solutions and Solvent at 25 °C from the X-ray Diffraction Measurements

	c (mol dm^{-3})				
solution	complex	solvent	d (g cm^{-3})	V (10^{-30} m^3)	μ (cm^{-1})
[Ru(acac)$_3$]	0.2540	17.65	0.826	6538	1.044
[Cr(acac)$_3$]	0.2538	17.64	0.813	6543	0.882
CH_3CN		18.91	0.777	6102[a]	0.474

[a] The volume including the same number of CH_3CN molecules as that in V for the [Ru(acac)$_3$] solution.

B. X-ray Diffraction Experiments. The sample of [Cr(acac)$_3$] was prepared as described in the previous section. Tris(acetylacetonato)ruthenium(III), [Ru(acac)$_3$], obtained from Aldrich Chemical Co. Inc. was purified chromatographically (alumina/C_6H_6), and the sample was dried under a reduced pressure for a few days after chromatographic purification. Spectroscopic-grade acetonitrile (Dojindo Laboratories) was used for the measurements of the solutions and reagent grade acetonitrile (Wako Pure Chemical Industries) for that of the neat solvent. Water contents in acetonitrile used were less than 13 mol m^{-3}. Concentration and other parameters for the solutions and solvent are summarized in Table 2.

The X-ray diffraction measurements were made at $2\theta = 1.6$−140° with a Rigaku $\theta-\theta$ diffractometer using Mo Kα radiation ($\lambda = 0.7107 \times 10^{-10}$ m) and a focusing LiF single-crystal monochromator at 26 ± 1 °C, in the same manner as described previously.[6] In the present study, the change of the effective scattering angle from the geometrical one due to the low absorption of solutions was corrected by estimating the position giving half of the observed scattering intensity. After the absorption correction, the diffraction intensity data were treated by a version of the KURVLR program modified for use on an IBM personal computer.[5,6]

IV. Results and Discussion

A. NMR Relaxation Study. *Concentration Dependence of $R_{1,obs}$.* The ^{1}H relaxation rates, $R_{1,obs}(^1H)$, of CH_3CN in [Cr(acac)$_3$]−CH_3CN solutions were determined as a function of the complex concentration, c, at three temperatures (Table 3); the methyl-^{13}C relaxation rates, $R_{1,obs}$(methyl-^{13}C), and the cyano-^{13}C relaxation rates, $R_{1,obs}$(cyano-^{13}C), were also determined (Tables 4 and 5, respectively). As seen in typical plots (Figure 2), $R_{1,obs}$ increases with c almost linearly, but the data points at higher concentration deviate slightly upward from linearity. This nonlinear dependence is rationalized as follows.

Substitution of eqs 9 and 14 into eq 3 gives

$$R_{1,obs} = K_I\left\{\frac{2N}{5c_s r^6}\tau_r + \frac{8\pi}{75}\frac{N_A}{dD_t}\right\}c + R_1^{dia} \quad (21)$$

TABLE 3: $R_{1,obs}$(^{1}H) of CH_3CN in $[Cr(acac)_3]-CH_3CN$ Solutions (s^{-1})[a]

	T (K)		
sample number	278.9	298.8	318.7
0	0.073(3)	0.066(2)	0.061(1)
1	2.55(8)	1.94(2)	1.47(8)
2	4.84(9)	3.62(5)	2.77(3)
3	8.43(3)	6.25(2)	4.85(15)
4	13.0(2)	9.68((5)	7.57(4)
5	15.3(6)	11.5(3)	
6	19.3(3)	14.4(3)	10.9(3)
7	28.0(4)	20.7(3)	15.7(4)
8	37.2(5)	27.5(3)	21.1(8)

[a] The 95% confidence limit in the least significant digits is given in parentheses.

TABLE 4: $R_{1,obs}$(methyl-^{13}C) of CH_3CN in $[Cr(acac)_3]-CH_3CN$ Solutions (s^{-1})[a]

	T (K)		
sample number	278.9	298.8	318.7
0	0.048(1)	0.047(1)	0.050(2)
1	0.192(6)	0.156(3)	0.128(6)
2	0.327(2)	0.256(2)	0.212(13)
3	0.532(3)	0.410(3)	0.325(30)
4	0.801 (32)	0.603 (10)	0.493(13)
5	0.925(49)	0.711(19)	
6	1.18(5)	0.858(25)	0.685(46)
7	1.66(5)	1.24(2)	0.978(36)
8	2.20(4)	1.59(2)	1.27(9)

[a] The 95% confidence limit in the least significant digits is given in parentheses.

Here, τ_r should be a linear function of *c*, as is the case of $[Co(acac)_3]$ in CH_3CN:[1]

$$\tau_r = \tau_r^{\infty}(1 + bc) \tag{22}$$

where τ_r^{∞} is the correlation time at infinite dilution. A similar expression is expected to hold for $1/D_t$, because this quantity should be proportional to the viscosity of the solution, which is linearly dependent on *c* as well. This coefficient for the concentration dependence of viscosity is usually denoted by *B*. If we identify *b* with *B* in analogy with the case of the cobalt complex,[1]

$$1/D_t = (1/D_t^{\infty})(1 + bc) \tag{23}$$

Inserting eqs 22 and 23 into eq 21 and rearranging, we have

$$R_{1,obs} = k_0 + k_1 c + k_2 c^2 \tag{24}$$

where

$$k_0 = R_1^{dia} \tag{25}$$

$$k_1 = K_1\left\{\frac{2N}{5c_s r^6}\tau_r^{\infty} + \frac{8\pi}{75}\frac{N_A}{dD_t^{\infty}}\right\} \tag{26}$$

and

$$k_2 = bk_1 \tag{27}$$

Since the variation of c_s is less than 3% for $c \leq 100$ mol m^{-3}, k_0, k_1, and k_2 are virtually independent of *c*.

The coefficients k_0, k_1, and k_2 are determined by fitting a quadratic equation to the data for $c \neq 0$ in Tables 3−5 at each temperature. They are presented in Tables 6−8. The solid lines in Figure 2 are best-fit regression curves.

TABLE 5: $R_{1,obs}$(cyano-^{13}C) of CH_3CN in $[Cr(acac)_3]-CH_3CN$ Solutions (s^{-1})[a]

	T (K)		
sample number	278.9	298.8	318.7
0		0.019(1)[b]	0.021(1)[c]
1	0.130(1)	0.104(3)	0.083(3)
2	0.230(16)	0.178(4)	0.143(8)
3	0.384(5)	0.302(7)	0.235(11)
4	0.601(2)	0.446(6)	0.358(4)
5	0.701(33)	0.524(23)	
6	0.879(40)	0.644(10)	0.512(11)
7	1.27(1)	0.937(45)	0.739(64)
8	1.66(3)	1.22(3)	0.965(63)

[a] The 95% confidence limit in the least significant digits is given in parentheses. [b] Determined at 299 K. [c] Determined at 319.2 ± 0.3 K.

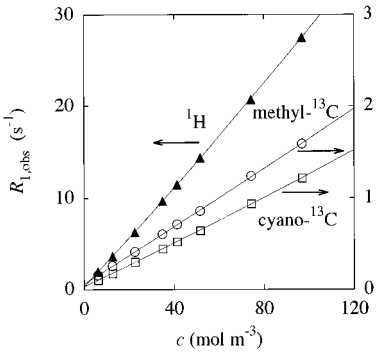

Figure 2. Variation of $R_{1,obs}$ of CH_3CN with *c* in $[Cr(acac)_3]-CH_3CN$ solutions at 298.8 K.

TABLE 6: k_0, k_1, and k_2 Obtained from $R_{1,obs}$(^{1}H) of CH_3CN in $[Cr(acac)_3]-CH_3CN$ Solutions[a]

T (K)	k_0 (s^{-1})	k_1 (s^{-1} dm^3 mol^{-1})	k_2 (s^{-1} dm^6 mol^{-2})	k_2/k_1 (dm^3 mol^{-1})
278.9	0.39(14)	341(7)	294(58)	0.86(19)
298.8	0.32(14)	261(7)	204(62)	0.78(26)
318.7	0.30(24)	204(12)	163(109)	0.80(58)

[a] The 95% confidence limit in the least significant digits is given in parentheses.

TABLE 7: k_0, k_1, and k_2 Obtained from $R_{1,obs}$(methyl-^{13}C) of CH_3CN in $[Cr(acac)_3]-CH_3CN$ Solutions[a]

T (K)	k_0 (s^{-1})	k_1 (10 s^{-1} dm^3 mol^{-1})	k_2 (10 s^{-1} dm^6 mol^{-2})	k_2/k_1 (dm^3 mol^{-1})
278.9	0.067(17)	1.98(8)	1.63(71)	0.82(39)
298.8	0.059(11)	1.55(5)	0.30(47)	0.20(31)
318.7	0.055(17)	1.25(10)	0.43(93)	0.34(77)

[a] The 95% confidence limit in the least significant digits is given in parentheses.

TABLE 8: k_0, k_1, and k_2 Obtained from $R_{1,obs}$(cyano-^{13}C) of CH_3CN in $[Cr(acac)_3]-CH_3CN$ Solutions[a]

T (K)	k_0 (s^{-1})	k_1 (10 s^{-1} dm^3 mol^{-1})	k_2 (10 s^{-1} dm^6 mol^{-2})	k_2/k_1 (dm^3 mol^{-1})
278.9	0.025(11)	1.58(6)	0.68(48)	0.43(32)
298.8	0.033(14)	1.16(7)	0.71(62)	0.61(57)
318.7	0.026(15)	0.95(8)	0.48(74)	0.51(82)

[a] The 95% confidence limit in the least significant digits is given in parentheses.

The value of k_0 should be equal to $R_{1,obs}$ observed in the absence of the paramagnetic complex. The agreement between these two values was within the experimental errors, except for the case of ^{1}H.

The k_2 values, as is expected from Figure 2, involve large uncertainties, and consequently so do the values of k_2/k_1. But the latter values scatter around the viscosity *B* coefficients of $[Co(acac)_3]$ in CH_3CN at these temperatures (0.7−0.8 dm^3

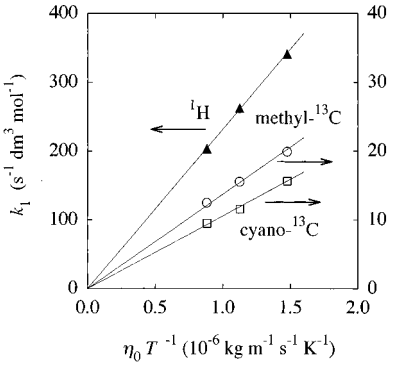

Figure 3. k_1 vs $\eta_0 T^{-1}$ for ^{1}H, methyl-^{13}C, and cyano-^{13}C in [Cr(acac)$_3$]−CH_3CN solutions.

TABLE 9: *P*(J) of ^{1}H and methyl-^{13}C in [Cr(acac)$_3$]−CH_3CN Solutions[a]

T (K)	^{1}H	methyl-^{13}C
278.9	1.37(7)	1.26(9)
298.8	1.42(12)	1.34(12)
318.7	1.36(19)	1.31(20)

[a] The 95% confidence limit in the least significant digits is given in parentheses.

mol^{-1}).[14] This observation indicates that the concentration dependence of $R_{1,obs}$ is expressed by eq 24.

The temperature dependence of k_1 arises mainly from τ_r^∞ and $1/D_t^\infty$. For [Co(acac)$_3$] in CH_3CN, τ_r^∞ was found to be proportional to the viscosity of pure solvent η_0 divided by temperature, and we explained this factor in terms of a model of rigid particles in a continuum fluid.[15] According to the same hydrodynamic model, $1/D_t^\infty$ is also proportional to $\eta_0 T^{-1}$. Consequently, k_1 is proportional to $\eta_0 T^{-1}$, if K_I, N, r, and d are independent of temperature. The plots in Figure 3 show that this is the case.

Estimation of r at a Given N. To determine r at a given N from k_1, K_I must be known. Unfortunately, exact evaluation of the values of K_I for [Cr(acac)$_3$] in solution is difficult. Therefore, we estimate r without the knowledge of K_I values in the following manner.

Equation 26 can be rewritten as

$$k_1(\mathrm{J})K_\mathrm{I}^{-1} = X_1 N\{r(\mathrm{J})\}^{-6} + X_2 \tag{28}$$

where

$$X_1 = \frac{2}{5c_s}\tau_r^\infty \quad \text{and} \quad X_2 = \frac{8\pi}{75}\frac{N_A}{dD_t^\infty} \tag{29}$$

This equation holds for each of the three observed nuclei of CH_3CN. The nucleus of interest is indicated by J: J = CN for the cyano-^{13}C, J = CH_3 for the methyl-^{13}C, and J = H for the protons. In eq 28, r(J) is the distance between the chromium atom and the specified nucleus of a bound CH_3CN molecule, and the values of X_1, X_2, and N are common to the three nuclei. By taking one of the three nuclei, say the cyano-^{13}C, as a reference, the relative value P(J) of k_1(J)/K_I for either of the remaining two is expressed by

$$P(\mathrm{J}) = \frac{k_1(\mathrm{J})/K_\mathrm{I}}{k_1(\mathrm{CN})/K_\mathrm{C}} = \frac{\{r(\mathrm{J})\}^{-6}X_1N + X_2}{\{r(\mathrm{CN})\}^{-6}X_1N + X_2}$$

$$(\mathrm{J} = \mathrm{CH_3 \text{ and } H}) \tag{30}$$

Because $K_I/K_C = (\gamma_I/\gamma_C)^2$, the values of P(J) are readily obtained from the data of Tables 6−8. They are listed in Table 9. The fact that P(H) and $P(CH_3)$ are larger than unity indicates that the methyl groups of the bound CH_3CN are preferentially oriented toward the complex.

To estimate X_1 and X_2, we assume that τ_r^∞ and D_t^∞ can be replaced by the corresponding values[15,16] for the [Co(acac)$_3$]−CH_3CN system (these values are included in Table 10). The distance of closest approach d of the nucleus of free CH_3CN molecules will be somewhat larger than the radius of the periphery of the complex molecule, which will lie at about 6×10^{-10} m from the central atom according to the crystal structure[17,18] of [Cr(acac)$_3$]. We arbitrarily chose a value of 7×10^{-10} m as d. This choice is not very important: r is rather insensitive to d, as seen from eq 30, in which the first term on the right-hand side depends on $1/\{r(\mathrm{J})\}^6$ and the second on $1/d$.

With the X_1 and X_2 values known, P(J) determines the relationship between r(CN) and r(J) for J = CH_3 and J = H if N is given. The two distances of $r(CH_3)$ and r(CN) can be related by the following explicit equation (Figure 4):

$$r(\mathrm{CN}) = [\{r(\mathrm{CH_3})\}^2 - 2ar(\mathrm{CH_3})\cos\varphi + a^2]^{1/2}$$

$$a = 1.43 \times 10^{-10}\ \mathrm{m} \tag{31}$$

Here, φ is the angle between the C_3 axis of CH_3CN and the $r(CH_3)$ vector and a is the bond length between the methyl and cyano carbons of the CH_3CN molecule determined by X-ray diffraction (see section B). It is impossible to give similar equation(s) for the methyl protons, because their configuration with respect to the chromium atom is not known. Therefore, we omit P(H) from further discussion.

Introducing eq 31 into eq 30, we obtain an equation containing three unknowns: N, $r(CH_3)$, and φ. For a given N, the values of $r(CH_3)$ and φ can be obtained by means of a graphical method. With a given N, $P(CH_3)$ is obtained as a function of $r(CH_3)$ for a value of φ, and a group of curves are drawn by changing φ from 90° to 180° (some exemplary curves for $N = 2$ are reproduced in Figure 5). On each curve, the $r(CH_3)$ coordinate that gives the observed $P(CH_3)$ value is read. In this way, the combinations of $r(CH_3)$ and φ consistent with the experimental data are obtained, giving an $r(CH_3)$ vs φ curve. The curves for $N = 2$, 4, and 5 are given in Figure 6, where the curve for $N = 4$ is accompanied by the confidence limits (broken lines) calculated from the uncertainty of $P(CH_3)$ (Table 9). The effect of temperature is small with respect to the experimental errors involved in the $P(CH_3)$ values. Once $r(CH_3)$ is known, φ can be estimated for a given N.

B. X-ray Diffraction Study. *Structure of the Complexes in Solutions.* Experimental radial distribution functions, $D(r)$, are given in Figure 7 as an expression of $D(r) - 4\pi r^2\rho_0$. Figure 8 shows the differences of $D(r)$ between either complex solution and the pure solvent ($\Delta D(r)$), roughly reflecting the correlation concerning the metal complexes. Three distinct peaks in $\Delta D(r)$ attributable to oxygen and carbon atoms of the ligands were found for $r \leq 4.5 \times 10^{-10}$ m. Their peak positions were not completely the same for the two solutions. Accordingly, the radial distribution function around the metal atom, $D^M(r)$, obtained by the isomorphous substitution procedure and shown in Figure 9, was analyzed by introducing somewhat different r(M−q) distances for the complexes into eq 20. The Ru−O and Cr−O bond lengths obtained were 2.01×10^{-10} and 1.97×10^{-10} m, in agreement with $2.004(14) \times 10^{-10}$ and $1.962(6) \times 10^{-10}$ m in the crystals,[4,18] respectively. The number of oxygen atoms per one metal atom, n_O, was 6.0(2), consistent with its stoichiometric number. The r(M−C(1)), r(M−C(2)), and r(M−C(3)) distances, obtained by assuming $n_C = 6$, 3, and 6, respectively, and summarized in Table 11, were essentially not different from the distances in the crystals: 2.902(14) for Ru−C(1), 3.232(15) for Ru−C(2), 4.267(17) for Ru−C(3) and

TABLE 10: X_1, X_2, and Values of Parameters in Eq 29

T (K)	c_s (mol dm^{-3})	τ_r^{∞} [a] (10^{-11} s)	D_t^{∞}(complex)[b] (10^{-10} m^2 s^{-1})	D_t^{∞}(AN)[b] (10^{-10} m^2 s^{-1})	X_1 (10^{-16} m^3 s mol^{-1})	X_2 (10^{40} m^{-3} s mol^{-1})
278.9	19.42	2.60	11.1	33.0	5.36	13.1
298.8	18.89	1.89	15.0	43.3	4.00	9.89
318.7	18.39	1.40	19.4	54.9	3.05	7.76

[a] From ref 15. [b] From ref 16.

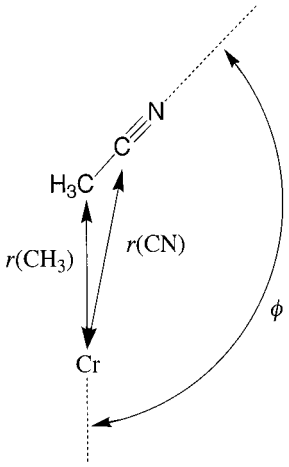

Figure 4. ϕ, $r(CH_3)$, and $r(CN)$.

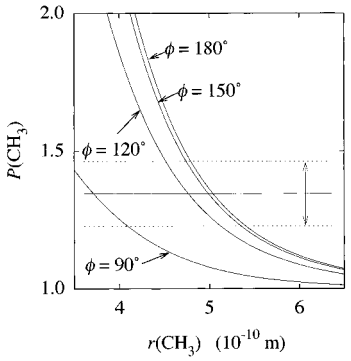

Figure 5. $P(CH_3)$ calculated as a function of $r(CH_3)$ at several ϕ for $N = 2$. The horizontal line is the experimental result of $P(CH_3) = 1.34$ with the 95% confidence limits shown by broken lines.

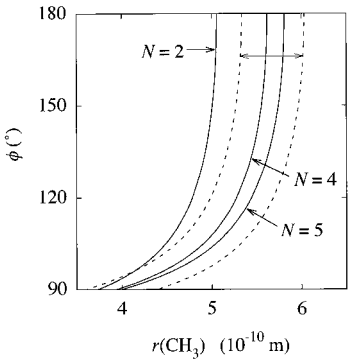

Figure 6. Relationships between ϕ and $r(CH_3)$ for $N = 2$, 4 (with the 95% confidence limits, broken curves), and 5.

2.896(10) for Cr−C(1), 3.253(16) for Cr−C(2), 4.243(12) for Cr−C(3) (in 10^{-10} m).[4,18] This similarity suggests that the structure of the complexes remains practically unchanged in acetonitrile. Figure 9 includes the theoretical curves calculated using the structure parameters (Table 11), where the r(M−H) distances were assumed to be 4.14×10^{-10} m for H(2) and 4.35×10^{-10}, 4.59×10^{-10}, and 4.88×10^{-10} m for H(3) analogously to those in the crystal,[4] and the values of l(M−H) were assumed to be $0.1_4 \times 10^{-10}$ m (the theoretical curve shape was little affected by assumed values of l(M−H)).

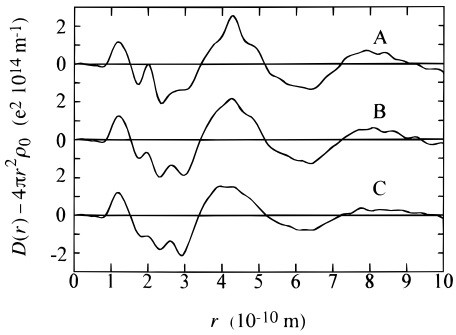

Figure 7. Structure-dependent part of $D(r)$: (A) [Ru(acac)$_3$] solution; (B) [Cr(acac)$_3$] solution; (C) pure acetonitrile.

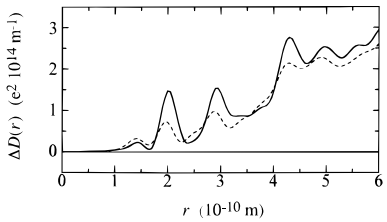

Figure 8. Difference in $D(r)$ between the complex solution and pure acetonitrile: (solid line) [Ru(acac)$_3$] solution; (dashed line) [Cr(acac)$_3$] solution.

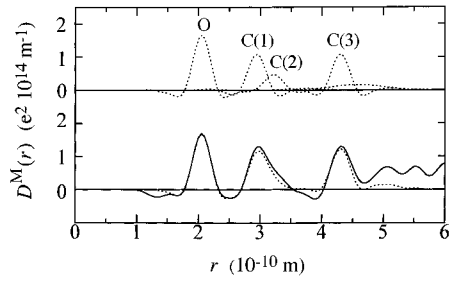

Figure 9. Experimental $D^M(r)$ curve (solid line), the theoretical curves calculated with the structure parameters given in Table 11 (upper dotted lines), and the sum of the theoretical curves (lower dotted line). The axis of ordinates is scaled with the scattering factor of ruthenium.

TABLE 11: Intramolecular Structure Parameters of [Ru(acac)$_3$] and [Cr(acac)$_3$] in Acetonitrile

correlation	r (10^{-10} m) M = Ru	r (10^{-10} m) M = Cr	l (10^{-10} m)
M−O	2.01(1)	1.97(1)	0.05(1)
M−C(1)	2.92(2)	2.90(3)	0.06(1)
M−C(2)[a]	3.23(3)	3.25(4)	0.10(3)
M−C(3)	4.28(2)	4.26(4)	0.06(2)

[a] Estimated by assuming the relation of r(Ru−C(2)) < r(Cr−C(2)) observed in the crystals[4,18] holds in the solutions as well, since the corresponding peak in $D^M(r)$ was not discrete.

Distribution of the Solvent Molecules around the Complexes. Figure 10 shows $D^M(r)_{os}$, which was obtained by eliminating the intramolecular correlation from $D^M(r)$. The contribution by solvent molecules appears beyond about 4×10^{-10} m, which is significantly shorter than 6×10^{-10} m, corresponding to the maximum distance from the metal atom to the molecular surface. This fact indicates the penetration of solvent molecules into the hollows on the surface formed by three acetylacetonato ligands.

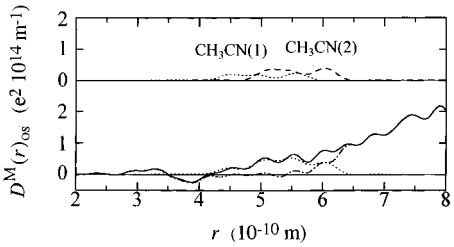

Figure 10. $D^M(r)_{os}$ (solid line) obtained by eliminating the intramolecular correlation from $D^M(r)$, the theoretical curves for $CH_3CN(1)$ (upper dotted line) and $CH_3CN(2)$ (dashed line), the sum of these theoretical curves (lower dotted line), and the difference between $D^M(r)_{os}$ and this sum (chain line). The axis of ordinates is scaled with the scattering factor of ruthenium.

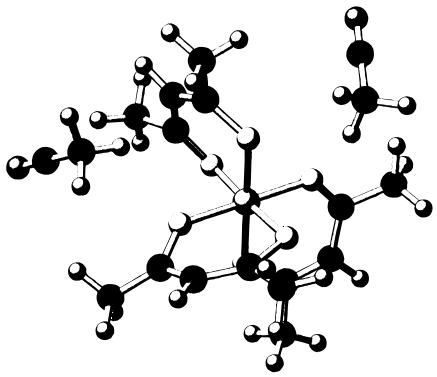

Figure 11. One of the possible locations of $CH_3CN(1)$ and $CH_3CN(2)$ in the hollows of the complex. The distances between the solvent molecules and the ligands are arbitrary as far as $r(M-C_{Me})$ and ϕ are the values in Table 12.

In the range of the distance up to 7×10^{-10} m, there is no particular distinct peak, but a mild bending around $r = 6 \times 10^{-10}$ m. This suggests the presence of specific solvent molecules distinguishable from bulk solvent molecules within 6×10^{-10} m. The curve in this region could not be reproduced by single-state solvent molecules.

An analysis was made to give a best fit to $D^M(r)_{os}$ in the range $r = 4-6 \times 10^{-10}$ m by assuming two types of solvent molecules, $CH_3CN(1)$ and $CH_3CN(2)$, and considering the condition of $r(M-C_{Me}) < r(M-C_{CN})$ obtained from the NMR study. The intramolecular structure parameters used for acetonitrile were as follows. The $C_{Me}-C_{CN}$ and $C_{CN}-N$ bond lengths were taken as $1.43(2) \times 10^{-10}$ m and $1.13(2) \times 10^{-10}$ m, respectively, obtained by the analysis of $D(r)$ for the pure solvent given in Figure 7C; these values were respectively close to $1.427(35) \times 10^{-10}$ and $1.114(14) \times 10^{-10}$ m in the crystal of $MgCl_2 \cdot 2SbCl_3 \cdot 6CH_3CN$[19] but somewhat different from $1.47(2) \times 10^{-10}$ and $1.15(1) \times 10^{-10}$ m, previously reported for the pure solvent.[20] The differences of the bond lengths between the present results and ref 20 are probably due to angle corrections made for the experimental data in the present study. The $C_{Me}-H$ bond length was taken as 1.1×10^{-10} m and the $H-C_{Me}-C_{CN}$ angle as 109.5°. The values of $l(M-C_{Me})$, $l(M-C_{CN})$, and $l(M-N)$ were taken as 0.14×10^{-10} m and $l(M-H)$ as 0.24×10^{-10} m. The differences between $r(Ru-q)$ and $r(Cr-q)$ were ignored in this analysis. The results are summarized in Table 12, and the theoretical curves are shown in Figure 10.

The $CH_3CN(1)$ molecules probably occupy the hollows along the C_3 axis, the $CH_3CN(2)$ molecules along the three C_2 axes.

TABLE 12: Locations of the CH_3CN Molecules in the Hollows of the Complex

$CH_3CN(i)$	$N(i)$	$r(M-C_{Me})$ (10^{-10} m)	ϕ (deg)
$CH_3CN(1)$	1.5(5)	4.5(1)	100(3)
$CH_3CN(2)$	2.5(5)	5.1(1)	98(3)

The angle of ϕ around 100° means that these solvent molecules lie almost in contact with the ligands in each hollow. The possibility of this situation was stereochemically confirmed by use of a CAChe molecular modeling system with computer graphics, considering the molecular structure data in the crystal.[4] It seemed natural that the methyl hydrogen atoms were in contact with oxygen atoms of the acetylacetonato ligands. One of the possible locations of $CH_3CN(1)$ and $CH_3CN(2)$ in the hollows is given in Figure 11. The numbers of the $CH_3CN(1)$ and $CH_3CN(2)$ molecules were $N(1) = 1.5(5)$ and $N(2) = 2.5(5)$, less than 2 and 3 for the hollows along the C_3 and C_2 axes, respectively. Such an incomplete filling may be needed to allow the exchange of the solvent molecules with bulk solvent molecules.

In view of the similarity of ϕ angles between $CH_3CN(1)$ and $CH_3CN(2)$ molecules, the results of the NMR study present some average of these two states. A weighted average of the $r(M-C_{Me})$ distances for the $CH_3CN(1)$ and $CH_3CN(2)$ molecules (Table 12) was calculated by the relation $r = [\{N(1) + N(2)\}/\{N(1)r(M-q)^{-6} + N(2)r(M-q)^{-6}\}]^{1/6}$. The result was $4.8_1 \times 10^{-10}$ m. For the $r(M-C_{CN})$ distances, the weighted average was $5.2_3 \times 10^{-10}$ m. These two values give 99(3)° for ϕ, in reasonable agreement with $\phi = 102(9)°$ at $r(M-C_{Me}) = 4.8 \times 10^{-10}$ m estimated from the curve for $N = 4$ (Figure 6) based on the value of P(methyl-^{13}C) in the NMR study.

References and Notes

(1) Kanakubo, M.; Ikeuchi, H.; Satô, G. P. *J. Magn. Reson.* **1995**, *A112*, 13.
(2) Kanakubo, M.; Ikeuchi, H.; Satô, G. P. *J. Mol. Liq.* **1995**, *65/66*, 273.
(3) Chao, G. K.-J.; Sime, R. L.; Sime, R. J. *Acta Crystallogr.* **1973**, *B29*, 2845.
(4) Matsuzawa, H.; Ohashi, Y.; Kaizu, Y.; Kobayashi, H. *Inorg. Chem.* **1988**, *27*, 2981.
(5) Johansson, G.; Yokoyama, H. *Inorg. Chem.* **1990**, *29*, 2460.
(6) Yokoyama, H.; Suzuki, S.; Goto, M.; Shinozaki, K.; Abe, Y.; Ishiguro, S. *Z. Naturforsch.* **1995**, *50a*, 301.
(7) Grahn, H.; Edlund, U.; Levy, G. C. *J. Magn. Reson.* **1984**, *56*, 61, and references cited therein.
(8) Abragam, A. *The Principles of Nuclear Magnetism*; Oxford University: Oxford, 1961; Chapter VIII.
(9) About the Debye approximation, see: McConnell, J. *The Theory of Nuclear Magnetic Relaxation in Liquids*; Cambridge University: Cambridge, 1987.
(10) Hexem, J. G.; Edlund, U.; Levy, G. C. *J. Chem. Phys.* **1976**, *64*, 936.
(11) McGarvey, B. R. *J. Phys. Chem.* **1957**, *61*, 1232.
(12) Hubbard, P. S. *Proc. R. Soc. London* **1966**, *A291*, 537.
(13) Endo, A.; Hoshino, Y.; Hirata, K.; Takeuchi, Y.; Shimizu, K.; Furushima, Y.; Ikecuhi, H.; Satô, G. P. *Bull. Chem. Soc. Jpn.* **1989**, *62*, 709.
(14) Ikeuchi, H.; Satô, G. P. *Abstract of Papers*, 24th IUPAC Conference on Solution Chemistry, Lisboa, 1995; Abstract PA01.
(15) Kanakubo, M. Ph.D. Thesis, Sophia University, 1996.
(16) Ikeuchi, H.; Satô, G. P. *Abstract of Papers*, 17th Symposium on Solution Chemistry of Japan, Okayama; Association of Japanese Solution Chemists, 1994; Abstract 2P07.
(17) Morosin, B. *Acta Crystallogr.* **1965**, *19*, 131.
(18) Kuroda, R.; Mason, S. F. *J. Chem. Soc., Dalton Trans.* **1979**, 273.
(19) Drew, M. G. B.; Claire, P. P. K.; Willey, G. R. *J. Chem. Soc., Dalton Trans.* **1988**, 215.
(20) Radnai, T.; Itoh, S.; Ohtaki, H. *Bull. Chem. Soc. Jpn.* **1988**, *61*, 3845.